



A PTHrP Gradient Drives Mandibular Condylar Chondrogenesis via Runx2

C. Tsutsumi-Arai¹, Y. Arai¹, A. Tran¹, M. Salinas¹, Y. Nakai¹ ,
S. Orikasa¹ , W. Ono¹ , and N. Ono¹ 

Abstract

The mandibular condylar cartilage (MCC) is an essential component of the temporomandibular joint, which orchestrates the vertical growth of the mandibular ramus through endochondral ossification with distinctive modes of cell differentiation. Parathyroid hormone-related protein (PTHrP) is a master regulator of chondrogenesis; in the long bone epiphyseal growth plate, PTHrP expressed by resting zone chondrocytes promotes chondrocyte proliferation in the adjacent layer. However, how PTHrP regulates chondrogenesis in the MCC remains largely unclear. In this study, we used a *Pthrp-mCherry* knock-in reporter strain to map the localization of PTHrP⁺ cells in the MCC and define the function of PTHrP in the growing mandibular condyle. In the postnatal MCC of *Pthrp^{mCherry/+}* mice, PTHrP-mCherry was specifically expressed by cells in the superficial layer immediately adjacent to RUNX2-expressing cells in the polymorphic layer. PTHrP ligands diffused across the polymorphic and chondrocyte layers where its cognate receptor PTH1R was abundantly expressed. We further analyzed the mandibular condyle of *Pthrp^{mCherry/mCherry}* mice lacking functional PTHrP protein (PTHrP-KO). At embryonic day (E) 18.5, the condylar process and MCC were significantly truncated in the PTHrP-KO mandible, which was associated with a significant reduction in cell proliferation across the polymorphic layer and a loss of SOX9⁺ cells in the chondrocyte layers. The PTHrP-KO MCC showed a transient increase in the number of Col10a1⁺ hypertrophic chondrocytes at E15.5, followed by a significant loss of these cells at E18.5, indicating that superficial layer-derived PTHrP prevents premature chondrocyte exhaustion in the MCC. The expression of *Runx2*, but not *Sp7*, was significantly reduced in the polymorphic layer of the PTHrP-KO MCC. Therefore, PTHrP released from cells in the superficial layer directly acts on cells in the polymorphic layer to promote proliferation of chondrocyte precursor cells and prevent their premature differentiation by maintaining *Runx2* expression, revealing a unique PTHrP gradient-directed mechanism that regulates MCC chondrogenesis.

Keywords: mandibular condylar cartilage (MCC), temporomandibular joint, articular cartilage, chondrocytes, periosteum, bone development

Introduction

The mandibular condylar cartilage (MCC) is primarily responsible for the vertical growth of the mandibular ramus and constitutes an essential component of the temporomandibular joint (TMJ) (Mizoguchi et al. 2013; Bender et al. 2018). The MCC undergoes endochondral ossification through distinctive modes of cell differentiation, which is often described as a secondary cartilage that entails chondrogenic conversion of the periosteum (Robinson et al. 2015; Bechtold et al. 2019). Functionally, the MCC adapts to the midface growth and masticatory forces (Hinton 2014). The MCC is composed of 4 distinct layers, including the superficial, polymorphic, flattened chondrocyte, and hypertrophic chondrocyte layer (Shibata et al. 1997; Bechtold et al. 2019). Among these layers, the polymorphic layer houses chondrocyte precursor cells that differentiate into hypertrophic chondrocytes in the deeper layers (Rabie and Hägg 2002; Rabie et al. 2003; Bechtold et al. 2019). Consequently, proliferation of chondrocyte precursor cells controls the rate of generating hypertrophic chondrocytes (Kantomaa et al. 1994; Robinson et al. 2015). This process of cellular differentiation makes the polymorphic layer pivotal to the growth of the mandibular condylar process and endows the MCC with substantial functional adaptability.

The parathyroid hormone-related protein (PTHrP) is a master regulator of chondrogenesis that promotes proliferation of chondrocytes and inhibits their hypertrophic differentiation (Schipani et al. 1997). PTHrP binds to its cognate receptor, the PTH/PTHrP receptor (PTH1R), which activates its downstream G protein-coupled receptor signaling (Kronenberg 2006). A previous study reports that *Pthrp* messenger RNA (mRNA) is present in the polymorphic layer of the MCC (Shibukawa et al. 2007) and regulates chondrocytes in the flattened layer. The early study demonstrates that chondrocyte proliferation is reduced in the MCC of PTHrP-deficient mice (Suda et al. 1999). In the epiphyseal growth plate, resting zone chondrocytes generate clones of columnar chondrocytes (Mizuhashi et al. 2018). In contrast, chondrocytes in the flattened layer differentiate rapidly into hypertrophic chondrocytes (Shibata

¹University of Texas Health Science Center at Houston School of Dentistry, Houston, TX, USA

A supplemental appendix to this article is available online.

Corresponding Author:

N. Ono, University of Texas Health Science Center at Houston School of Dentistry, 1941 East Rd., Houston, TX 77054, USA.
Email: noriaki.ono@uth.tmc.edu

et al. 2006) without generating distinct columns of chondrocytes, indicating that a unique mechanism of chondrocyte proliferation and differentiation exists in the MCC. However, the precise source of PTHrP and how PTHrP promotes chondrogenesis in the MCC remains largely undefined. In addition, the target gene of PTHrP in the polymorphic layer has not been identified.

In this study, we aimed to determine the identity of cells expressing PTHrP in the MCC and define how PTHrP regulates chondrogenesis in the MCC. Our findings demonstrate that PTHrP derived from the superficial layer promotes MCC chondrogenesis by regulating *Runx2* expression in the polymorphic layer, revealing a unique PTHrP gradient-directed mechanism of chondrogenesis in the MCC.

Materials and Methods

Mouse Strains

Pthrp-mCherry knock-in reporter mice have been previously described (Mizuhashi et al. 2018). Briefly, the native start codon in exon 2 of the *Pthrp* gene was replaced with a *Kozak-mCherry-bGHpA* cassette using CRISPR/Cas9 genome editing. All mice were housed in the animal facility accredited by the Association for Assessment and Accreditation of Laboratory Animal Care, located in the Behavioral and Biological Sciences Building of the University of Texas Health Science Center at Houston. All procedures were conducted in compliance with the Guide for the Care and Use of Laboratory Animals and approved by the University of Texas Health Science Center at Houston's Animal Welfare Committee (AWC), protocol AWC-21-0070. We have complied with the ARRIVE (Animal Research: Reporting of In Vivo Experiments) 2.0 guidelines. More detailed protocols for mouse management are available in the Appendix Materials and Methods.

For postnatal experiments, male *Pthrp^{mCherry/+}* mice were mated to female C57BL/6 mice and their pups were sacrificed at postnatal day (P) 3. For prenatal experiments, male *Pthrp^{mCherry/+}* mice were mated to female *Pthrp^{mCherry/+}* mice and the vaginal plug was checked in the morning. Pregnant mice were sacrificed at embryonic day (E) 15.5 or E18.5. Pups and fetuses were used for analysis regardless of the sex. A total of 16 pregnant female mice and 72 fetuses were used for the experiments. No statistical method was used to predetermine sample size. Mice were euthanized by overdosage of inhalation anesthesia in a drop jar (Fluriso, Isoflurane USP; VetOne) followed by decapitation.

Histology

Samples were fixed in 4% paraformaldehyde for 24 h at 4°C. P3 samples were decalcified in 15% EDTA for 3 h. Samples were cryoprotected in 30% sucrose/phosphate-buffered saline (PBS) solutions and then in 30% sucrose/PBS:optimal cutting temperature (OCT) compound (1:1) solutions, each at least overnight at 4°C. Samples were embedded in an OCT compound (Tissue-Tek; Sakura). Frozen sections at 12 μm

thickness were prepared using a cryostat (Leica CM1860) and adhered on positively charged glass slides (Fisherbrand ColorFrost Plus).

RNAscope In Situ Hybridization and Immunohistochemistry

In situ hybridization was performed with an RNAscope Multiplex Fluorescent Detection Reagents v2 kit (Advanced Cell Diagnostics 323110) using the following probes: *Col10a1* (426181), *Runx2* (414021), *Pth1r* (426191), *Ihh* (413091), and *Sp7* (403401). After RNAscope, sections were incubated in blocking buffer (3% bovine serum albumin/Tris-buffered saline with Tween (TBST)) for 30 min at room temperature (RT), and subsequently stained with SOX9 polyclonal antibody (1:500; R&D systems, AF3075), RUNX2 polyclonal antibody (1:100; Novus Biological, NBP1-89104), PTHrP polyclonal antibody (1:100; Invitrogen, PA5-57493), PTH1R monoclonal antibody (3D1.1) (1:200; Novus Biological, NBP1-40067), DsRed Polyclonal Antibody (Living Colors) (1:700; Takara Bio, 632496), or mCherry monoclonal antibody (16D7) (1:400; Invitrogen, M11217), overnight at 4°C. Sections were subsequently stained with appropriate Alexa Fluor-conjugated secondary antibodies for 3 h at 4°C, followed by DAPI (4',6-diamidino-2-phenylindole, 5 μg/mL; Invitrogen D1306) staining. More detailed experimental procedures are available in the Appendix Materials and Methods.

Signal Quantification for RNAscope on Images

Quantification of RNAscope fluorescent signals on sections was performed using Fiji software (version 2.9.0). A 100-μm × 100-μm square was set on the polymorphic layer in microscopic images, and the expression level of a gene was calculated within the square in pixels. The expression level was represented as pixels per μm².

Statistical Analysis

Results are presented as mean values ± SD. Statistical evaluation was conducted using the unpaired *t* test or 1-way analysis of variance (ANOVA) followed by Tukey's honestly significant difference multiple comparison test. A *P* value of <0.05 was considered significant.

Results

PTHrP Is Expressed in the Superficial Layer Adjoining RUNX2⁺SOX9^{neg} Cells in the Polymorphic Layer

First, we mapped the localization of PTHrP⁺ cells across the postnatal mandible using *Pthrp-mCherry* knock-in reporter mice (Mizuhashi et al. 2018). In the *Pthrp-mCherry* allele, red fluorescent protein mCherry is expressed instead of a functional PTHrP protein, constituting a null reporter allele (Fig. 1A). *Pthrp^{mCherry/+}* mice carry 1 functional copy of PTHrP and

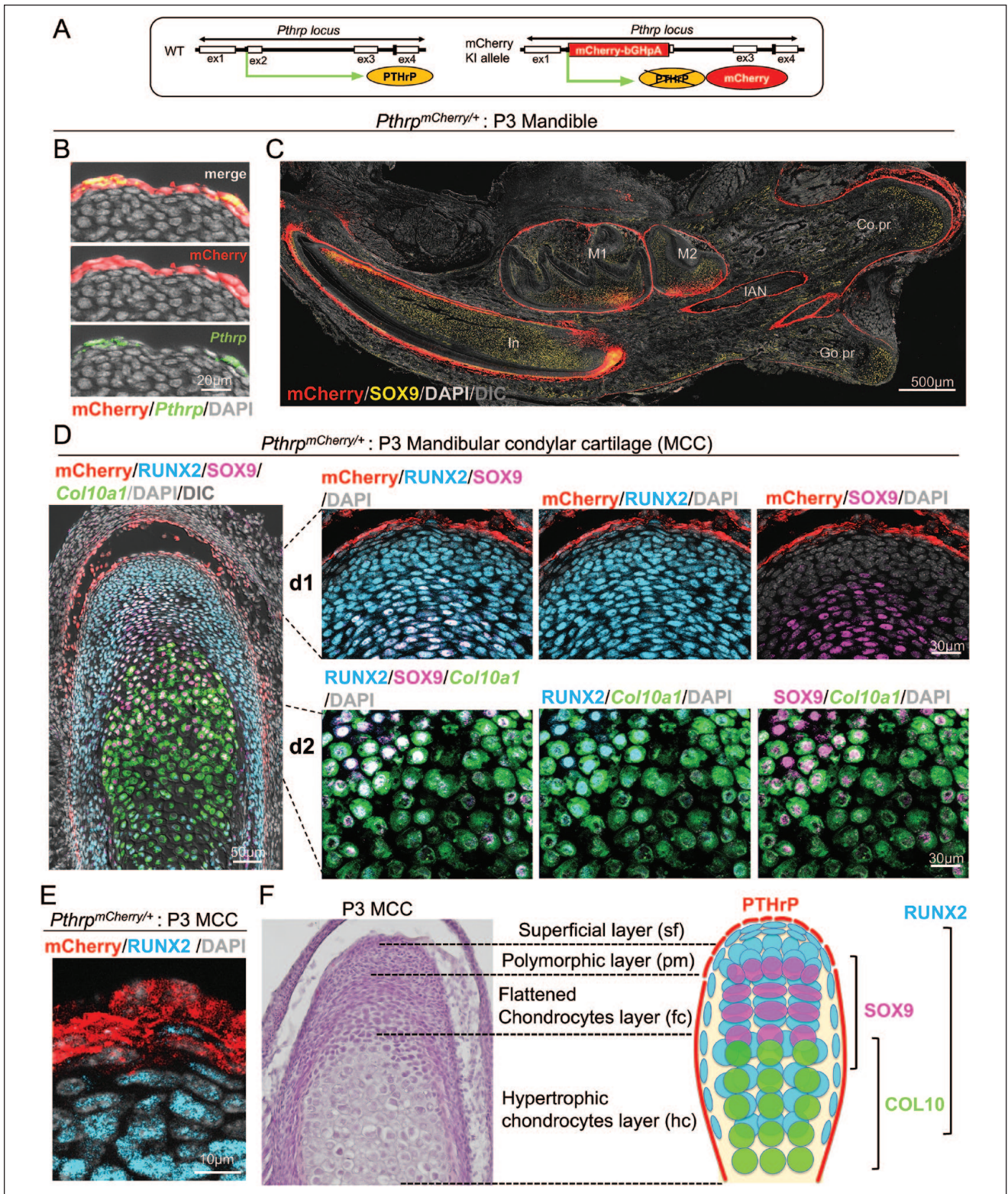


Figure 1. Parathyroid hormone–related protein (PTHrP) is expressed in the superficial layer adjoining RUNX2⁺SOX9^{neg} cells in the polymorphic layer. **(A)** Structure of *Pthrp*-mCherry knock-in allele. In *Pthrp*-mCherry allele, red fluorescent protein mCherry is expressed instead of a functional PTHrP protein, constituting a null reporter allele. **(B, C)** Sagittal section of *Pthrp*^{mCherry/+} mandible at postnatal day 3 (P3). **(B)** Magnified view of mandibular condylar cartilage (MCC). *Pthrp* messenger RNA RNAscope assay (in situ hybridization [ISH]). Scale bar: 20 μm. **(C)** Overview of the mandible. Co.pr, condylar process; Go.pr, gonial process; IAN, inferior alveolar nerve; In, incisor; M1, first molar; M2, second molar. Red: PTHrP-mCherry (IHC), yellow: SOX9-Alexa647 (IHC), gray: DAPI. Scale bar: 500 μm. *n* = 4 mice. **(D, E)** *Pthrp*^{mCherry/+} MCC at P3. **(D)** Scale bar: 50 μm. **(d1)** Magnified view of the superficial, polymorphic, and flattened chondrocyte layers. **(d2)** Magnified view of the hypertrophic chondrocytes layer. Red: PTHrP-mCherry (IHC), blue: RUNX2-Alexa647 (IHC), magenta: SOX9-Alexa750 (IHC), green: *Col10a1*-Opal520 (ISH), gray: DAPI. Scale bars: 30 μm. *n* = 4 mice. **(E)** Magnified view of MCC. Scale bar: 10 μm. **(F)** Hierarchical structure of MCC at P3, hematoxylin and eosin staining (left) and diagram (right) highlighting PTHrP, RUNX2, SOX9, and *Col10a1* expression.

1 copy of mCherry and are phenotypically indistinguishable from wild-type mice. Importantly, PTHrP-mCherry recapitulates the endogenous expression pattern of *Pthrp* mRNA, providing a sensitive and convenient readout of *Pthrp* gene expression. (Fig. 1B, Appendix Fig. 1A).

At P3, PTHrP-mCherry⁺ cells were preferentially localized in a manner surrounding SOX9⁺ cells in the mandible (Fig. 1C). Particularly in the dentoalveolar compartment, PTHrP-mCherry⁺ cells occupied the dental follicle surrounding growing incisor and molars, as well as the dental epithelium in the labial cervical loop of the incisor, as reported previously (Sharir et al. 2019; Takahashi et al. 2019; Nagata et al. 2021). Interestingly in the posterior compartment, PTHrP-mCherry⁺ cells occupied the entire surface of the condylar process but not the gonial process (Fig. 1C). SOX9⁺ cells in these processes were chondrocytes, as they were embedded in Safranin O⁺ cartilaginous matrices (Appendix Fig. 1B).

We closely examined the precise location of PTHrP-mCherry⁺ cells in the MCC. PTHrP-mCherry⁺ cells were localized to the superficial layer, occupying 2 to 3 cell layers on the surface of the MCC (Fig. 1D, E), in a more restricted pattern than what was previously reported using radioactive in situ hybridization (Shibukawa et al. 2007; Bechtold et al. 2019). No *Pthrp* mRNA RNAscope signal was observed in the deeper layers (Fig. 1B, Appendix Fig. 1A). PTHrP-mCherry⁺ cells were also localized to the forming temporomandibular joint disc as well as the fibrous region of the forming glenoid fossa (Fig. 1C). The PTHrP-mCherry⁺ cells in the superficial layer adjoined RUNX2⁺SOX9^{neg} cells in the polymorphic layer (Fig. 1DK–d1, E). Cells in the polymorphic layer underwent robust proliferation, as indicated by the presence of EdU⁺ cells in this layer (Appendix Fig. 1C). Importantly, essentially all SOX9⁺ cells in the flattened chondrocyte layer coexpressed RUNX2 (Fig. 1D–d1), denoting the unique characteristics of MCC chondrocytes. Col10a1⁺ cells in the upper hypertrophic layer were RUNX2⁺SOX9⁺, while those in the lower hypertrophic layer were negative for both RUNX2 and SOX9 (Fig. 1D–d2). This difference indicates that MCC chondrocytes lose RUNX2 and SOX9 expression during terminal stages of differentiation.

We next asked if PTHrP ligands released from the superficial layer act on the polymorphic and chondrocyte layers of the MCC. For this purpose, we performed PTHrP immunohistochemistry on PTHrP-mCherry⁺ sections, which gives a simultaneous readout of *Pthrp* mRNA by PTHrP-mCherry and PTHrP protein (Appendix Fig. 1D). Robust PTHrP immunohistochemical signal was observed in the polymorphic and flattened chondrocyte layers but not in the hypertrophic chondrocyte layer (Appendix Fig. 1D, left panel). Interestingly, PTHrP was predominantly detected on the cell surface in the polymorphic layer, whereas it was also detected intracellularly in the flattened chondrocyte layer (Appendix Fig. 1E), indicating an organized diffusion of PTHrP ligands. Immunostaining revealed that PTH1R was abundantly expressed in the polymorphic and flattened chondrocyte layers by RUNX2⁺ cells (Appendix Fig. 1D, right panel, Appendix Fig. 1F). Therefore, these data indicate that PTHrP released from the superficial layer diffuses across the MCC and binds to its cognate receptor

PTH1R on RUNX2⁺ and SOX9⁺ cells in the polymorphic and flattened chondrocyte layer. This diffusion process emanates biological actions by activating PTHrP-PTH1R signaling in cells in the polymorphic and chondrocyte layers, supporting the model that PTHrP stands atop the hierarchical structure of the MCC (Fig. 1F). PTHrP produced by the superficial layer of the lateral side also likely plays an important role in regulating the polymorphic layer.

PTHrP Promotes MCC Chondrogenesis and Mandibular Condyle Formation

We next set out to determine the functional significance of superficial layer–derived PTHrP in the mandibular condylar morphogenesis and MCC chondrogenesis. To this end, we analyzed littermates of *Pthrp*^{mCherry/+} (Control) and *Pthrp*^{mCherry/mCherry} (PTHrP-KO) mice at E18.5. Of note, *Pthrp*^{mCherry/mCherry} mice lacked functional PTHrP protein but expressed 2 copies of mCherry reporter proteins in cells that were supposed to express *Pthrp* mRNA (Fig. 2A). Importantly, PTHrP immunoreactivity was completely absent in *Pthrp*^{mCherry/mCherry} mice (Fig. 2B, left panel), confirming the loss of functional PTHrP protein in PTHrP-KO MCC. There was no notable alternation in the expression pattern of PTH1R in PTHrP-KO MCC (Fig. 2B right panel). Therefore, we postulated that an organized diffusion of PTHrP ligands is essential for promoting MCC chondrogenesis, consistent with the concept that morphogen gradient regulates organogenesis (Fig. 2C) (Gurdon and Bourillot 2001).

We performed 3-dimensional micro-computed tomography (3D- μ CT) analysis of Control and PTHrP-KO mandibles at E18.5 (Fig. 2D, left panel). Importantly, the length and width of the condylar process were significantly reduced in the PTHrP-KO mandible (Fig. 2D, red arrows in left and middle panels). In contrast, the length of the gonial process was not altered in the PTHrP-KO mandible (Fig. 2D, green arrows in left and right panels). Therefore, PTHrP specifically promotes mandibular condylar morphogenesis, which corroborates our finding that PTHrP⁺ cells are present on the surface of the condylar process but not on the gonial process.

We further performed skeletal staining of Control and PTHrP-KO mandibles. Alcian Blue⁺ cartilaginous tissues were substantially diminished in the condylar process but not in the gonial process of the PTHrP-KO mandible (Fig. 2E, left panel). Additionally, Safranin O staining on sections revealed that the cartilage length was significantly reduced in the condylar process of the PTHrP-KO mandible (Fig. 2F). Therefore, PTHrP plays major functional roles in promoting MCC chondrogenesis and the formation of the mandibular condyle.

PTHrP Promotes Cell Proliferation in the Polymorphic Layer and Formation of SOX9⁺ Chondrocytes

To identify the cause of the significant defects observed in the PTHrP-KO mandibular condyle, we next evaluated cell proliferation of the polymorphic layer at 2 distinct stages of condylar

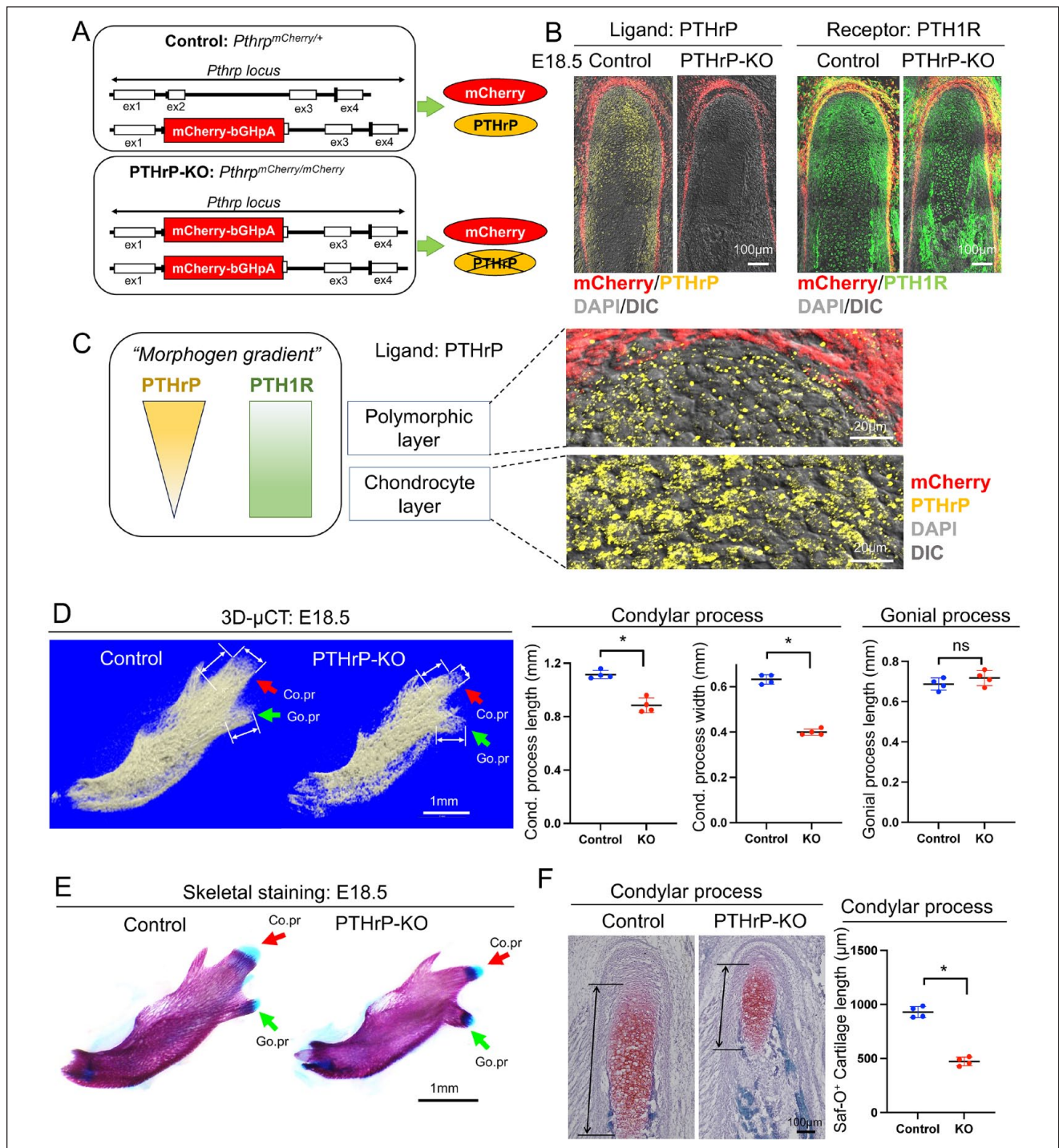


Figure 2. Parathyroid hormone-related protein (PTHrP) promotes mandibular condylar cartilage (MCC) chondrogenesis and mandibular condyle formation. **(A)** *Pthrp* locus of Control (*Pthrp*^{mCherry/+}) and PTHrP-KO (*Pthrp*^{mCherry/mCherry}) mice. **(B)** Expression of the ligand (PTHrP) and the receptor (PTH1R) at E18.5. Left: PTHrP, right: PTH1R. Red: PTHrP-mCherry (in situ hybridization [ISH]), yellow: PTHrP-Alexa647 (IHC), green: PTH1R-Alexa647 (IHC), gray: DAPI. Scale bars: 100 µm. *n* = 4 mice. **(C)** Diagram of PTHrP ligand gradient regulating MCC chondrogenesis. Right panels: magnified views of PTHrP immunoreactivity, polymorphic (upper) and chondrocyte (lower) layers. Scale bars: 20 µm. **(D)** Three-dimensional micro-computed tomography of Control and PTHrP-KO mandibles at E18.5. Red arrow: condylar process, green arrow: gonial process. Scale bar: 1 mm. Right: quantification of the length and width of the condylar and gonial process. *n* = 4 mice per each group. Two-tailed, unpaired *t* test. Data are presented as mean ± SD. A *P* value of <0.05 was considered significant. **(E)** Skeletal staining of Control and PTHrP-KO mandibles at E18.5. Red arrow: condylar process, green arrow: gonial process. Scale bar: 1 mm. *n* = 4 mice. **(F)** Safranin O staining of Control and PTHrP-KO MCC. Scale bar: 100 µm. Right: quantification of the cartilage length (double-headed arrows). *n* = 4 mice per each group. Two-tailed, unpaired *t* test. Data are presented as mean ± SD. A *P* value of <0.05 was considered significant. **P* < 0.05, ns: not significant.

morphogenesis—one stage at E15.5 when the MCC is specified, as well as another stage at E18.5 when the MCC growth is most prominent (see Fig. 3A for hematoxylin and eosin [H&E] staining). Cell proliferation defined by EdU was significantly reduced in the polymorphic layer of the PTHrP-KO MCC at both E15.5 and E18.5 (Fig. 3B). At higher magnification, most of the reduction in EdU⁺ cells within the PTHrP-KO MCC occurred in the polymorphic layer occupied by RUNX2⁺ cells; the reduction in EdU⁺ cells was more prominent at E18.5 (Fig. 3C). Therefore, PTHrP derived from the superficial layer preferentially regulates proliferation of RUNX2⁺ cells in the polymorphic layer.

We also quantified the length of SOX9⁺ domains in the PTHrP-KO mandibular condyle. Interestingly, no difference was observed at E15.5; however, there was a significant reduction in the SOX9⁺ domain in the PTHrP-KO MCC at E18.5 (Fig. 3D). Therefore, PTHrP does not regulate the initial specification of chondrocyte precursors in the early MCC but promotes continuous growth of the MCC in later stages, presumably through maintaining proliferation of chondrocyte precursor cells in the polymorphic layer.

PTHrP Prevents Premature Chondrocyte Differentiation and Exhaustion

The significant loss of SOX9⁺ chondrocytes observed in the E18.5 PTHrP-KO MCC promoted us to investigate the late-stage markers of chondrocyte differentiation. To this end, we first examined the expression of a canonical hypertrophic chondrocyte marker, Col10a1. While no difference in the SOX9⁺ domain between the Control and PTHrP-KO was noted at E15.5 (Fig. 3C), the Col10a1⁺ domain was significantly expanded in the PTHrP-KO at the same stage (Fig. 4A, left panel), indicating that MCC chondrocytes undergo premature hypertrophy in the absence of PTHrP. In contrast, the Col10a1⁺ domain was significantly reduced in the PTHrP-KO at E18.5, indicating that a lack of PTHrP depletes chondrocyte precursor cells in the polymorphic layer and subsequently reduces hypertrophic chondrocytes.

We also analyzed the expression of *Ihh*, which is a classical target gene of PTHrP in the growth plate. In early development of the long bone growth plate, PTHrP released from the periarticular layer inhibits *Ihh* expression in the prehypertrophic layer (Karaplis et al. 1994; St-Jacques et al. 1999). In line with this, the *Ihh*⁺ domain was expanded in the PTHrP-KO MCC compared to the Control at E15.5 (Fig. 4B, left panel). Interestingly, however, the *Ihh*⁺ domain was markedly diminished in the PTHrP-KO MCC at E18.5 (Fig. 4B, right panel), indicating that superficial layer–derived PTHrP is required to maintain *Ihh* expression in MCC chondrocytes. Therefore, PTHrP prevents premature differentiation of SOX9⁺ chondrocytes to Col10a1⁺ hypertrophic chondrocytes during active MCC growth, while also positively regulating *Ihh* expression from prehypertrophic chondrocytes, highlighting a unique mechanism of MCC chondrogenesis.

PTHrP Preferentially Promotes Runx2 Expression in the Polymorphic Layer

The polymorphic layer of the MCC develops from the periosteum of the mandibular ramus during early condylar morphogenesis and maintains its contiguity with the periosteum in the postnatal mandibular condylar process (Shibata et al. 2013; Kurio et al. 2018). Therefore, we examined the expression of transcription factors Runx2 and Sp7 (encoding Osterix) in the polymorphic layer, which are essential for osteoblast differentiation. Importantly, both *Runx2* and *Sp7* were abundantly expressed in the polymorphic layer at both E15.5 and 18.5 (Fig. 5A–a1,2). In the PTHrP-KO MCC, *Runx2* expression was significantly reduced at both E15.5 and 18.5 (Fig. 5A–a1), while *Sp7* expression was not altered (Fig. 5A–a2). These findings support the notion that Runx2 in the adjacent polymorphic layer may be an immediate target of PTHrP derived from the superficial layer of the MCC.

Taken together, our findings support the model that, in the MCC, PTHrP released from the superficial layer of the MCC acts on cells in the polymorphic layer, promotes proliferation of chondrocyte precursor cells in the polymorphic layer, and prevents their premature differentiation by stimulating Runx2 expression through the PTHrP-PTH1R signaling pathway (Fig. 5B). Of note, Runx2 has been shown to be required for chondrocyte proliferation in the postnatal MCC (Liao et al. 2019). A quantitative reduction in the RUNX2 functional activity causes cleidocranial dysplasia-like bone phenotype in mice (Lou et al. 2009) and may also induce the impairment in MCC chondrogenesis.

Discussion

In this study, we report that PTHrP is expressed in the superficial layer of the MCC and regulates the expression of *Runx2* in the adjacent polymorphic layer through an organized diffusion. PTHrP released from the superficial layer acts on RUNX2⁺ chondrocyte precursor cells in the adjacent polymorphic layer and promotes proliferation and differentiation of RUNX2⁺ precursor cells into SOX9⁺ chondrocytes (see Fig. 5B for the model of fetal MCC development). Consistent with the concept that morphogen gradient regulates organogenesis (Gurdon and Bourillot 2001), PTHrP ligands diffuse in an organized manner, localized predominantly on the cell surface in the polymorphic layer to bind to its cognate receptor PTH1R, and subsequently localize intracellularly in the chondrocyte layer, presumably through PTH1R internalization. Lack of PTHrP reduces *Runx2* expression in the MCC and inhibits proliferation of precursor cells in the polymorphic layer and accelerates differentiation of chondrocyte precursor cells to hypertrophic chondrocytes. As a result, lack of PTHrP causes defective endochondral bone formation of the mandibular condyle, associated with an altered zonal structure and the overall reduced size in the PTHrP-KO MCC. In other words, PTHrP-responsive Runx2 maintains cell proliferation of precursor cells in the polymorphic layer and prevents their premature terminal differentiation, which ultimately

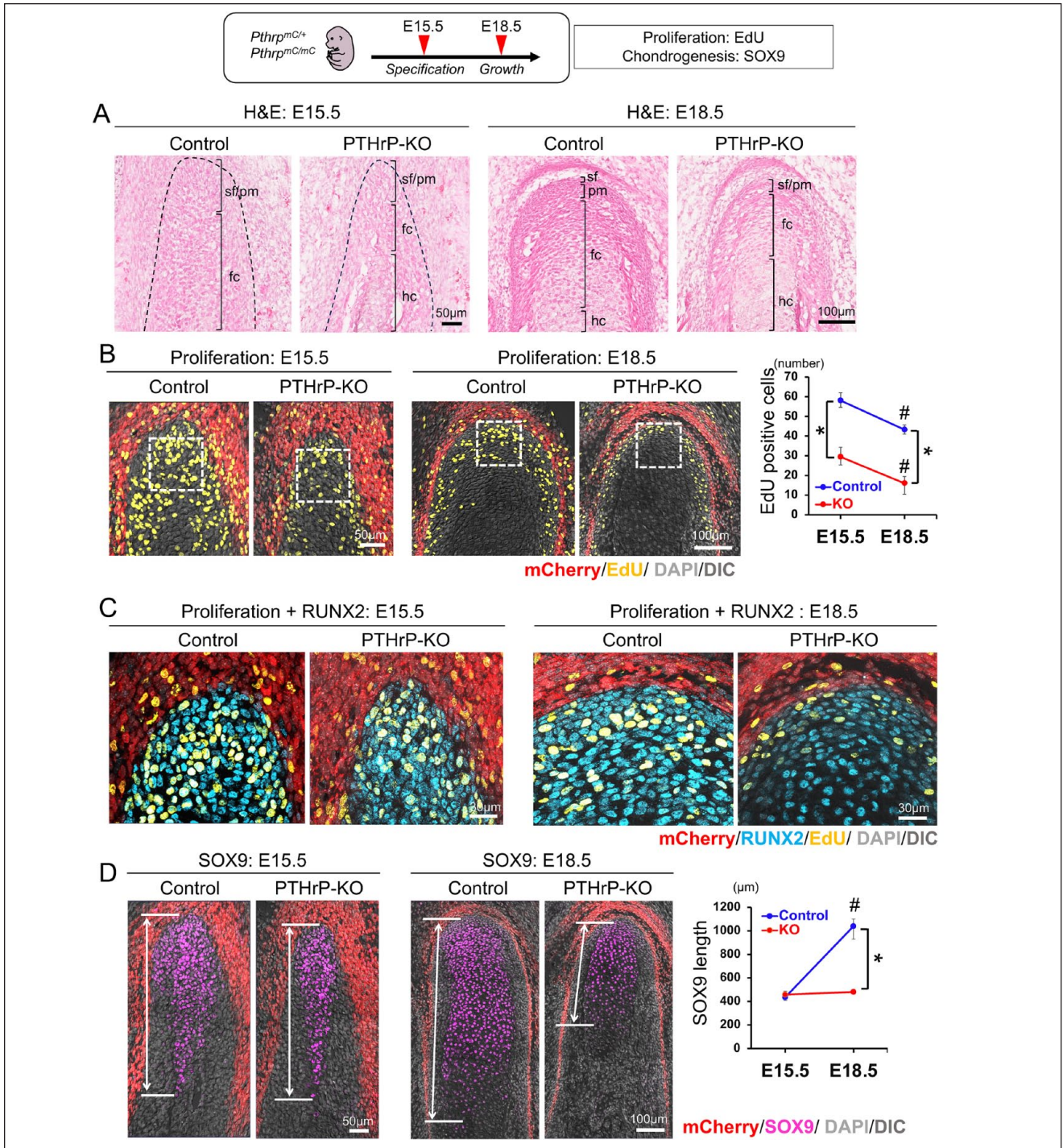


Figure 3. Parathyroid hormone–related protein (PTHrP) promotes cell proliferation in the polymorphic layer and formation of SOX9⁺ chondrocytes. **(A)** Hematoxylin and eosin (H&E) staining of Control (*Pthrp^{mCherry/+}*) and PTHrP-KO (*Pthrp^{mCherry/mCherry}*) mandibular condylar cartilage (MCC) at E15.5 and E18.5. fc, flattened chondrocyte; hc, hypertrophic chondrocyte; pm, polymorphic; sf, superficial. Scale bars: 50 μ m (E15.5), 100 μ m (E18.5). **(B)** Cell proliferation assay of Control (*Pthrp^{mCherry/+}*) and PTHrP-KO (*Pthrp^{mCherry/mCherry}*) MCC at E15.5 and E18.5 by EdU. White boxes (100 \times 100 μ m): areas used to quantify EdU⁺ cells. Red: PTHrP-mCherry (in situ hybridization [ISH]), yellow: EdU-Alexa480, gray: DAPI. Scale bars: 100 μ m. Right: quantification of EdU⁺ cells in the polymorphic layer. Blue line: Control, red line: PTHrP-KO. $n=4$ mice per each group. Two-tailed, 1-way analysis of variance (ANOVA) followed by Tukey's post hoc test. Data are presented as mean \pm SD. A P value of <0.05 was considered significant (* $P<0.05$: between Control and PTHrP-KO, # $P<0.05$: between E15.5 and E18.5). **(C)** Magnified views of the polymorphic layer highlighting EdU and RUNX2. Red: PTHrP-mCherry (IHC), blue: RUNX2-Alexa647 (IHC). Scale bars: 30 μ m. $n=4$ mice. **(D)** Length of SOX9⁺ domains (double-headed arrows) in Control and PTHrP-KO MCC at E15.5 and E18.5. Red: PTHrP-mCherry (IHC), magenta: SOX9-Alexa647 (IHC). Scale bars: 50 μ m (E15.5), 100 μ m (E18.5). Right: quantification of SOX9⁺ domain. Blue line: Control, red line: PTHrP-KO. SOX9⁺ domain is significantly reduced in PTHrP-KO MCC at E18.5. $n=4$ mice per each group. Two-tailed, 1-way ANOVA followed by Tukey's post hoc test. Data are presented as mean \pm SD. A P value of <0.05 was considered significant (* $P<0.05$: between Control and PTHrP-KO, # $P<0.05$: between E15.5 and E18.5).

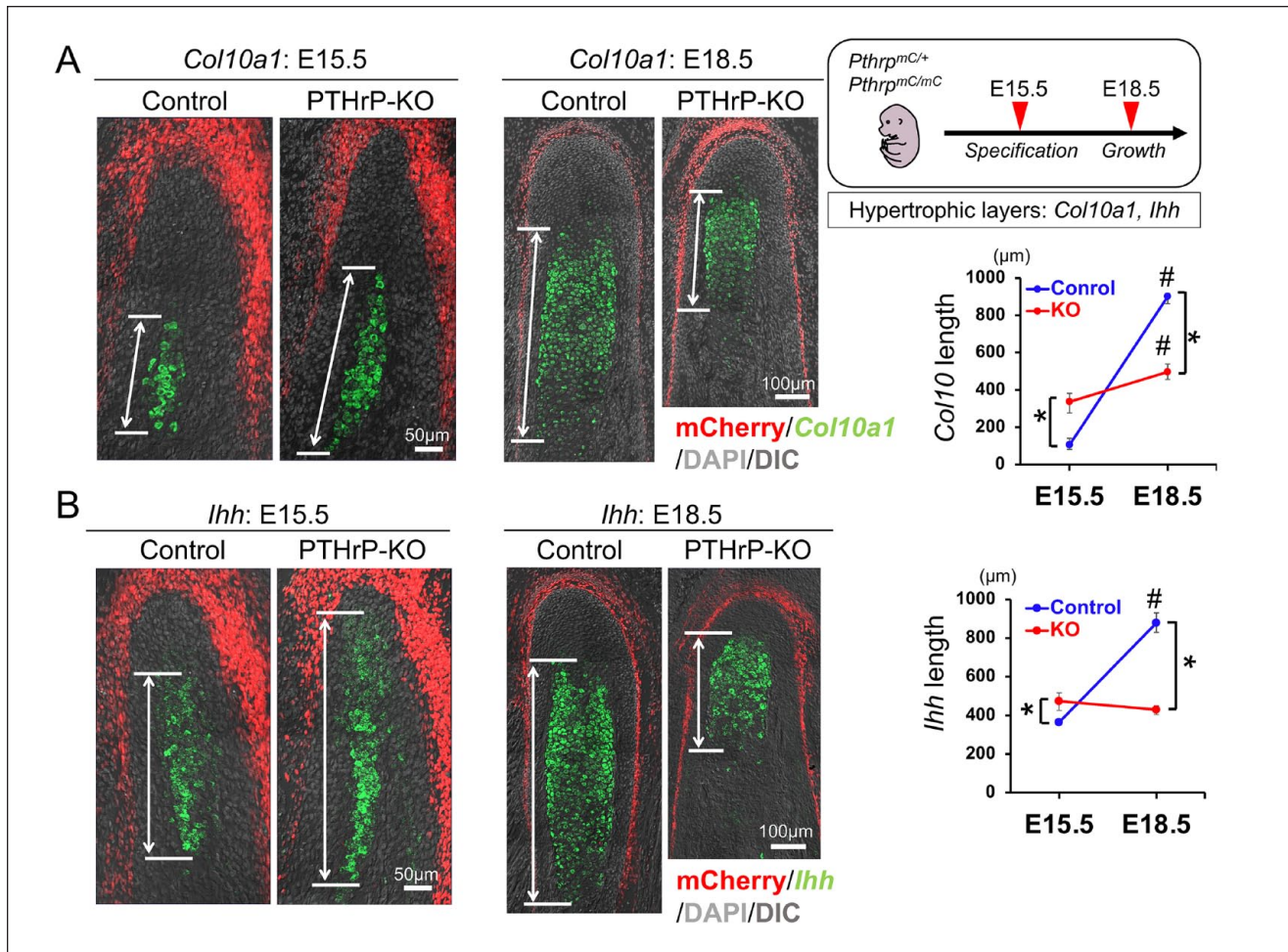


Figure 4. Parathyroid hormone-related protein (PTHrP) prevents premature chondrocyte differentiation and exhaustion. **(A)** *Col10a1* expression domain (double-headed arrows) in Control (*Pthrp*^{mCherry/+}) and PTHrP-KO (*Pthrp*^{mCherry/mCherry}) mandibular condylar cartilage (MCC) at E15.5 and E18.5. Red: PTHrP-mCherry (in situ hybridization [ISH]), green: *Col10a1*-Opal520 (ISH). Right: quantification of *Col10a1* expression domain (double-headed arrows). $n=4$ mice per each group. Two-tailed, 1-way analysis of variance (ANOVA) followed by Tukey's post hoc test. Data are presented as mean \pm SD. A P value of <0.05 was considered significant (* $P<0.05$: between Control and PTHrP-KO, # $P<0.05$: between E15.5 and E18.5). **(B)** *Ihh* expression domain (double-headed arrows) in Control and PTHrP-KO MCC at E15.5 and E18.5. Red: PTHrP-mCherry (IHC), green: *Ihh*-Opal520 (ISH). Right: quantification of *Ihh* expression domain (double-headed arrows). $n=4$ mice per each group. Two-tailed, one-way ANOVA followed by Tukey's post hoc test. Data are presented as mean \pm SD. A P value of <0.05 was considered significant (* $P<0.05$: between Control and PTHrP-KO, # $P<0.05$: between E15.5 and E18.5).

determines cartilage extension in the MCC. It has been previously reported that PTHrP-deficient mice show a reduction in thickness of all layers of the MCC (Suda et al. 1999). Although this observation is consistent with our present histologic examination, we have further clarified the mechanisms underlying this phenotype from 2 perspectives; first, PTHrP is expressed by the superficial layer and diffuses across the polymorphic and chondrocyte layers, and second, the reduction in the MCC thickness is due to accelerated differentiation and inhibition of cell proliferation, which is associated with reduced *Runx2* expression.

In long bones, the resting zone of the epiphyseal growth plate plays central roles in the proper development and growth of endochondral bones by housing a population of chondrocytes expressing PTHrP (Mizuhashi et al. 2018). The population is recognized as skeletal stem cells, defined by their ability to undergo self-renewal and clonally give rise to columnar

chondrocytes in the postnatal growth plate. These chondrocytes also possess the ability to differentiate into a multitude of cell types, including osteoblasts and bone marrow stromal cells, during skeletal development. It is not clear from the current study whether PTHrP⁺ cells in the superficial layer contribute to cells in other layers, including the polymorphic and chondrocyte layers of MCC. Unraveling the cell fate of PTHrP⁺ superficial layer cells in the MCC will facilitate our mechanistic understanding of MCC formation and maintenance.

In our study, although the detailed actions of PTHrP signaling in the MCC were not studied, we revealed the causal relationship between PTHrP and *Runx2* but not PTHrP and *Sp7* (Osterix). In the long bone, *Runx2* promotes chondrocyte hypertrophy, whereas PTHrP delays this process (Li et al. 2004; Yoshida et al. 2004; van der Horst et al. 2005; Zhang et al. 2009). It has been reported that PTHrP downregulates

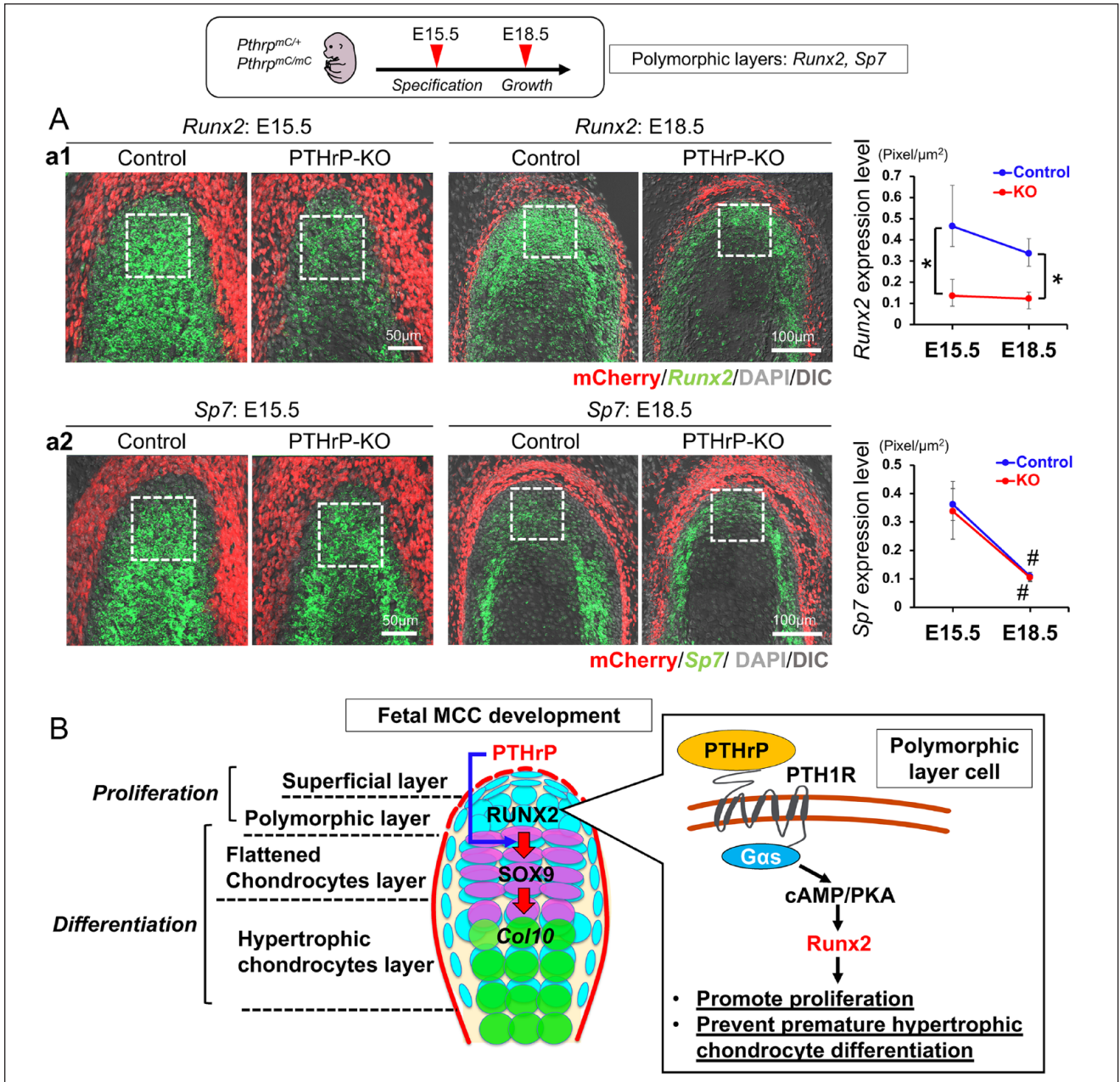


Figure 5. Parathyroid hormone–related protein (PTHrP) preferentially promotes *Runx2* expression in the polymorphic layer. **(A)** *Runx2* and *Sp7* (encoding Osterix) expression in Control (*Pthrp^{mCherry/+}*) and PTHrP-KO (*Pthrp^{mCherry/mCherry}*) mandibular condylar cartilage (MCC) polymorphic layer at E15.5 and E18.5. (a1) *Runx2* expression at E15.5 and 18.5. Red: PTHrP-mCherry (in situ hybridization [ISH]), green: *Runx2*-Opal520 (ISH). Right: quantification of *Runx2* expression level. (a2) *Sp7* expression at E15.5 and E18.5. Red: PTHrP-mCherry (IHC), green: *Sp7*-Opal520 (ISH). Right: quantification of *Sp7* expression level. *n* = 4 mice per each group. Two-tailed, 1-way analysis of variance followed by Tukey’s post hoc test. Data are presented as mean ± SD. A *P* value of <0.05 was considered significant (**P* < 0.05; between Control and PTHrP-KO, #*P* < 0.05; between E15.5 and E18.5). **(B)** Concluding diagram. PTHrP released from the superficial layer acts on cells in the polymorphic layer, promotes proliferation of chondrocyte precursor cells in the polymorphic layer, and prevents their premature differentiation by stimulating *Runx2* expression through the PTHrP-PTH1R signaling pathway.

Runx2 expression through the PKA signaling pathway in chick upper sternal chondrocytes (Li et al. 2004). PTHrP also prevents chondrocyte premature hypertrophy by inducing RUNX2 degradation in long bones in mice (van der Horst et al. 2005; Zhang et al. 2009). In other words, the action of *Runx2* on chondrocyte differentiation in the MCC appears to be opposite

to that of PTHrP in the long bone growth plate. Our results indicate that both PTHrP and *Runx2* have prochondrogenic functions, suggesting that there is a unique mechanism of chondrocyte proliferation and differentiation in the MCC.

In conclusion, our study identifies a unique mechanism by which PTHrP stimulates MCC formation by maintaining

Runx2 expression in chondrocyte precursor cells in the polymorphic layer through an organized diffusion. Modulating a PTHrP gradient within the MCC may provide a viable venue to intervene with the continual and adaptive growth of the MCC.

Author Contributions

C. Tsutsumi-Arai, N. Ono, contributed to conception, design, data acquisition, analysis, and interpretation, drafted and critically revised the manuscript; Y. Arai, contributed to conception, data acquisition and analysis, drafted and critically revised the manuscript; A. Tran, M. Salinas, contributed to data analysis, drafted and critically revised the manuscript; Y. Nakai, S. Orikasa, contributed to data acquisition, drafted and critically revised the manuscript; W. Ono, contributed to conception, design, data interpretation, drafted and critically revised the manuscript. All authors gave final approval and agree to be accountable for all aspects of the work.

Acknowledgments

We thank Dr. Catherine G. Ambrose (Department of Orthopedic Surgery at the University of Texas Health Science Center at Houston McGovern Medical School) for assistance in 3D-microCT scanning and Drs. Yoshihiro Komatsu and Hiroyuki Yamaguchi (Department of Pediatrics at the University of Texas Health Science Center at Houston McGovern Medical School) for assistance in skeletal staining.





Declaration of Conflicting Interests

The authors declared no potential conflicts of interest with respect to the research, authorship, and/or publication of this article.

Funding

The authors disclosed receipt of the following financial support for the research, authorship, and/or publication of this article: This work was supported by grants from the National Institutes of Health (R01DE030630, R01DE026666 to N. Ono and R01DE029181, R01DE030416 to W. Ono). C. Tsutsumi-Arai was supported by the Japan Society for the Promotion of Science Fellowship for Research Abroad.

ORCID iDs

Y. Nakai  <https://orcid.org/0000-0003-2695-6097>
 S. Orikasa  <https://orcid.org/0000-0002-4226-7358>
 W. Ono  <https://orcid.org/0000-0002-0358-1897>
 N. Ono  <https://orcid.org/0000-0002-3771-8230>

References

- Bechtold TE, Kurio N, Nah HD, Saunders C, Billings PC, Koyama E. 2019. The roles of Indian hedgehog signaling in TMJ formation. *Int J Mol Sci.* 20(24):6300.
- Bender ME, Lipin RB, Goudy SL. 2018. Development of the pediatric temporomandibular joint. *Oral Maxillofac Surg Clin North Am.* 30(1):1–9.
- Gurdon JB, Bourillot PY. 2001. Morphogen gradient interpretation. *Nature.* 413(6858):797–803.
- Hinton RJ. 2014. Genes that regulate morphogenesis and growth of the temporomandibular joint: a review. *Dev Dyn.* 243(7):864–874.
- Kantomaa T, Tuominen M, Pirttiniemi P. 1994. Effect of mechanical forces on chondrocyte maturation and differentiation in the mandibular condyle of the rat. *J Dent Res.* 73(6):1150–1156.
- Karaplis AC, Luz A, Glowacki J, Bronson RT, Tybulewicz VL, Kronenberg HM, Mulligan RC. 1994. Lethal skeletal dysplasia from targeted disruption of the parathyroid hormone-related peptide gene. *Genes Dev.* 8(3):277–289.
- Kronenberg HM. 2006. PTHrP and skeletal development. *Ann N Y Acad Sci.* 1068:1–13.
- Kurio N, Saunders C, Bechtold TE, Salhab I, Nah HD, Sinha S, Billings PC, Pacifici M, Koyama E. 2018. Roles of Ihh signaling in chondrogenitor function in postnatal condylar cartilage. *Matrix Biol.* 67:15–31.
- Li TF, Dong Y, Ionescu AM, Rosier RN, Zuscik MJ, Schwarz EM, O'Keefe RJ, Drissi H. 2004. Parathyroid hormone-related peptide (PTHrP) inhibits Runx2 expression through the PKA signaling pathway. *Exp Cell Res.* 299(1):128–136.
- Liao L, Zhang S, Zhou GQ, Ye L, Huang J, Zhao L, Chen D. 2019. Deletion of Runx2 in condylar chondrocytes disrupts TMJ tissue homeostasis. *J Cell Physiol.* 234(4):3436–3444.
- Lou Y, Javed A, Hussain S, Colby J, Frederick D, Pratap J, Xie R, Gaur T, van Wijnen AJ, Jones SN, et al. 2009. A Runx2 threshold for the cleidocranial dysplasia phenotype. *Hum Mol Genet.* 18(3):556–568.
- Mizoguchi I, Toriya N, Nakao Y. 2013. Growth of the mandible and biological characteristics of the mandibular condylar cartilage. *Jpn Dent Sci Rev.* 49(4):139–150.
- Mizuhashi K, Ono W, Matsushita Y, Sakagami N, Takahashi A, Saunders TL, Nagasawa T, Kronenberg HM, Ono N. 2018. Resting zone of the growth plate houses a unique class of skeletal stem cells. *Nature.* 563(7730):254–258.
- Nagata M, Chu AKY, Ono N, Welch JD, Ono W. 2021. Single-cell transcriptomic analysis reveals developmental relationships and specific markers of mouse periodontium cellular subsets. *Front Dent Med.* 2:679937.
- Rabie AB, Hägg U. 2002. Factors regulating mandibular condylar growth. *Am J Orthod Dentofacial Orthop.* 122(4):401–409.
- Rabie AB, Tang GH, Xiong H, Hägg U. 2003. PTHrP regulates chondrocyte maturation in condylar cartilage. *J Dent Res.* 82(8):627–631.
- Robinson J, O'Brien A, Chen J, Wadhwa S. 2015. Progenitor cells of the mandibular condylar cartilage. *Curr Mol Biol Rep.* 1(3):110–114.
- Schipani E, Lanske B, Hunzelman J, Luz A, Kovacs CS, Lee K, Pirro A, Kronenberg HM, Jüppner H. 1997. Targeted expression of constitutively active receptors for parathyroid hormone and parathyroid hormone-related peptide delays endochondral bone formation and rescues mice that lack parathyroid hormone-related peptide. *Proc Natl Acad Sci U S A.* 94(25):13689–13694.
- Sharif A, Marangoni P, Zilionis R, Wan M, Wald T, Hu JK, Kawaguchi K, Castillo-Azofeifa D, Epstein L, Harrington K, et al. 2019. A large pool of actively cycling progenitors orchestrates self-renewal and injury repair of an ectodermal appendage. *Nat Cell Biol.* 21(9):1102–1112.
- Shibata S, Fukada K, Suzuki S, Yamashita Y. 1997. Immunohistochemistry of collagen types II and X, and enzyme-histochemistry of alkaline phosphatase in the developing condylar cartilage of the fetal mouse mandible. *J Anat.* 191(Pt 4):561–570.
- Shibata S, Sato R, Murakami G, Fukuoka H, Francisco Rodríguez-Vázquez J. 2013. Origin of mandibular condylar cartilage in mice, rats, and humans: periosteum or separate blastema? *J Oral Biosci.* 55(4):208–216.
- Shibata S, Suda N, Suzuki S, Fukuoka H, Yamashita Y. 2006. An in situ hybridization study of Runx2, Osterix, and Sox9 at the onset of condylar cartilage formation in fetal mouse mandible. *J Anat.* 208(2):169–177.
- Shibukawa Y, Young B, Wu C, Yamada S, Long F, Pacifici M, Koyama E. 2007. Temporomandibular joint formation and condyle growth require Indian hedgehog signaling. *Dev Dyn.* 236(2):426–434.
- St-Jacques B, Hammerschmidt M, McMahon AP. 1999. Indian hedgehog signaling regulates proliferation and differentiation of chondrocytes and is essential for bone formation. *Genes Dev.* 13(16):2072–2086.
- Suda N, Shibata S, Yamazaki K, Kuroda T, Senior PV, Beck F, Hammond VE. 1999. Parathyroid hormone-related protein regulates proliferation of condylar hypertrophic chondrocytes. *J Bone Miner Res.* 14(11):1838–1847.
- Takahashi A, Nagata M, Gupta A, Matsushita Y, Yamaguchi T, Mizuhashi K, Maki K, Ruellas AC, Cevidanes LS, Kronenberg HM, et al. 2019. Autocrine regulation of mesenchymal progenitor cell fates orchestrates tooth eruption. *Proc Natl Acad Sci U S A.* 116(2):575–580.
- van der Horst G, Farih-Sips H, Löwik CW, Karperien M. 2005. Multiple mechanisms are involved in inhibition of osteoblast differentiation by PTHrP and PTH in KS483 cells. *J Bone Miner Res.* 20(12):2233–2244.
- Yoshida CA, Yamamoto H, Fujita T, Furuichi T, Ito K, Inoue K, Yamana K, Zanna A, Takada K, Ito Y, et al. 2004. Runx2 and Runx3 are essential for chondrocyte maturation, and Runx2 regulates limb growth through induction of Indian hedgehog. *Genes Dev.* 18(8):952–963.
- Zhang M, Xie R, Hou W, Wang B, Shen R, Wang X, Wang Q, Zhu T, Jonason JH, Chen D. 2009. PTHrP prevents chondrocyte premature hypertrophy by inducing cyclin-D1-dependent Runx2 and Runx3 phosphorylation, ubiquitylation and proteasomal degradation. *J Cell Sci.* 122(Pt 9):1382–1389.